Journal of Alloys and Compounds 503 (2010) 65–70

Contents lists available at ScienceDirect

Journal of Alloys and Compounds

journal homepage: www.elsevier.com/locate/jallcom

Influence of the addition of indium on the mechanical creep of Sn–3.5%Ag alloy

S.E. Negm [*,1], H. Mady [1], A.A. Bahgat

Department of Physics, Faculty of Science, Al-Azhar Univ., Nasr City 11884, Cairo, Egypt

ARTICLE INFO

Article history:
Received 28 April 2010
Accepted 2 May 2010
Available online 7 May 2010

Keywords:
Sn–Ag–In
Soldering
Creep
Microstructure

ABSTRACT

The present study was undertaken to investigate the influence of In metal addition to the eutectic Sn–3.5Ag binary composition for use as a Pb-free solder. The resulting properties of the binary system were extended to the Sn-based ternary systems Sn–Ag3.5–8In and Sn–Ag3.5–16In (where the composition are in wt.%) solder. Creep property and the microhardness tests of the Sn–Ag–In alloys were studied. The alloys showed the three creep stages. The activation energy for the steady state creep of the alloys was found to have an average value of 0.34 and 0.42 eV respectively. This might be characterizes by volume self diffusion as the controlling mechanism. On the other hand, the microstructures of the as cast alloys are reported as well. In addition the microstructure of the solder alloys before and after creep test was investigated.

© 2010 Elsevier B.V. All rights reserved.

1. Introduction

Lead metal free soldering alloys are an important issue in the protection against poisonous materials in the world environmental safety. Soldering technology has become indispensable for the interconnection and packaging of virtually all electronic devices and circuits. The Sn–Ag binary eutectic solder is one possible lead-free solder replacement for Sn–Pb. This alloy system is quite important because it is generally recognized as the first choice for lead-free solders. It is well characterized [1], and the eutectic composition and temperature are Sn–3.5 wt.% Ag and 494 K, respectively. It possesses good ductility and better creep and thermal resistance than Sn–Pb solders. Although Sn–Ag eutectic solder melts at 494 K compared to 458 K of Sn–Pb eutectic solder, this may be acceptable for high temperature applications [2]. The tin–silver eutectic alloy has already been used in electronics soldering to a limited extent [3]. In addition, it is used for soldering of stainless steel for food processing applications. The Sn–In and Sn–Ag investigated solder alloys are already in practical use, but only in exactly determined conditions. Considering these, it could be expected that Ag–In–Sn ternary system might be one among the proper substitutes for common solders [4].

Mechanical creep of a soldering material occurs more readily when elevated temperatures are involved. Since regions of inhomogeneous microstructural coarsening are known to be preferred sites for creep cracks to initiate, one of the keys to improved solder joint reliability is the ability to engineer and to stabilize fine, uniform microstructures. Also at elevated temperature, the mechanical properties of metals are a result of simultaneous processes of strain hardening, due to plastic deformation, and the softening effect of recovery and recrystallization [5].

The mechanical properties of binary alloys Sn–Ag, Sn–Sb and Sn–Zn have been studied by the present group [1,6–8]. The present motivation is to explore further the experimental findings made by this group and to illuminate some light on the effect of indium addition on these alloys soldering properties especially concerning creep test. In the present analysis, the creep parameters under the effect of five constant applied stresses were measured under different working temperatures for the Sn-based solder alloys. Furthermore, microhardness study was performed as well. The microstructure of the original as cast alloys was studied micrographically before and after creep test as well.

2. Experimental work

Two alloys samples of the compositions Sn–3.5Ag–8In and Sn–3.5Ag–16In in weight percent were prepared from 99.99% spc-pure elements. They were formed by melting the constituents in a Pyrex tube under a fluxing agent (Colophony) to prevent the sample oxidation in air. The melting was carried out on a benzene flame for more than 30 min while the tube was shaken to ensure homogenization of the melt. After solidification, the tube was broken to obtain the alloy. The density of the samples was measured by the displacement method using carbon tetrachloride (CCl_4) as the immersion liquid. The melting points of the alloys have been detected by homemade computerized differential thermal analysis (DTA) measurements.

Microhardness [9] tests were conducted using a Vickers hardness type Shimadzu tester applying a load of 25 g for 10 s by a Vickers diamond pyramid. Grinding and polishing were necessary to obtain polished, smooth and flat parallel surface before indentation tester. The readings of different indentations were taken at room temperature to obtain the mean value and the standard deviation was calculated. The creep specimens on the other hand of the two compositions Sn–3.5Ag–8In and Sn–3.5Ag–16In were swaged in the form of wires (diameter 0.66 mm) with

* Corresponding author. +20 2 1037 23604 (Mobile).
E-mail addresses: Samiadourgham@yahoo.com (S.E. Negm), alaabahgat@yahoo.com (A.A. Bahgat).
[1] Girls Branch.

0925-8388/$ – see front matter © 2010 Elsevier B.V. All rights reserved.
doi:10.1016/j.jallcom.2010.05.007

Table 1
Calculated density of the pewter alloys.

Wt.%	$\rho_{cal.}$ (g/cm^3)	$\rho_{exp.}$ (g/cm^3)
Sn–3.5Ag [1]	7.4	7.4
Sn–3.5Ag–8In	7.4	7.4
Sn–3.5Ag–16In	7.26	7.4

cold work of approximately 94.5%. The wire samples were annealed for 1 h at 324 ± 2K. Following heat treatment, the samples were allowed to cool slowly to room temperature with a rate of ≈0.04 K s^{-1}. Creep tests were carried out at different temperatures in the range from 443 to 483 K under different applied stresses ranging from 5.1 to 6.6 MPa using a homemade computer assisted creep machine [1,6–8].

All samples (bulk, wires before and after creep test) were polished, etched with a solution of 3 ml HNO_3–97 ml alcohol for about 5 s and washed by distilled water. Microphotographical examination of the structural changes of the specimens after heat treatment, cold work and the creep test was done. Metallography was performed using an optical microscope type (Carl Zeiss Jena) at different magnifications.

3. Results and discussion

The value of the bulk density was determined in the present work as given in Table 1, from which the porosity is determined to be less than 0.01%, proving the efficiency of the present preparation procedure.

3.1. Melting point

The thermal behavior of the solders was investigated using differential thermal analysis (DTA) at constant heating rate 10 °C/min. It is shown that there is only one phase transformation observed in the temperature range 303–533 K, namely the melting which is indicated by the endothermic peak. The melting points were considered in support of probable industrial applications. Fig. 1 shows that the eutectic temperature decreases gradually with higher In metal content. The eutectic temperature reaches about 473 K when the In content is 16 wt.%.

The effect of In addition on the eutectic temperature of the Sn–Ag binary system phase diagram reveals that the melting point of Sn–Ag is depressed [10] with the addition of In. In addition the melting range (temperature range between solidus and liquidus points according to DTA) is extended as indium metal addition. The onset temperature (the onset point of heat absorption during heating) was reduced from 494 K (Sn–3.5Ag) to 488 K (Sn–3.5Ag–8In) and 473 K (Sn–3.5Ag–16In) as shown in Fig. 2. Therefore the addition of 16 wt.% indium metal to the binary alloy Sn–3.5Ag reduced the working melting point to approach that of the common Sn–Pb soldering alloy.

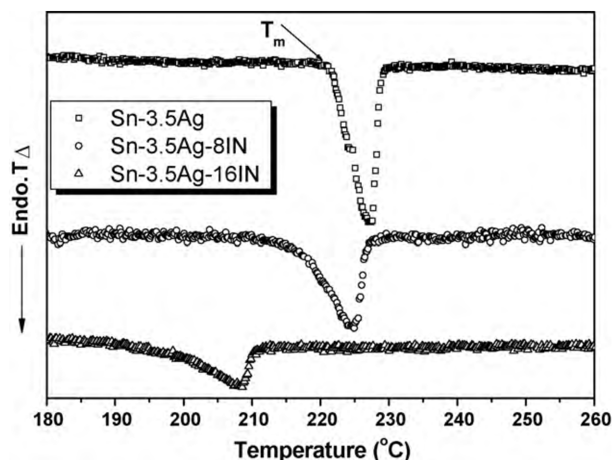

Fig. 1. DTA measurements of the Sn solder alloys.

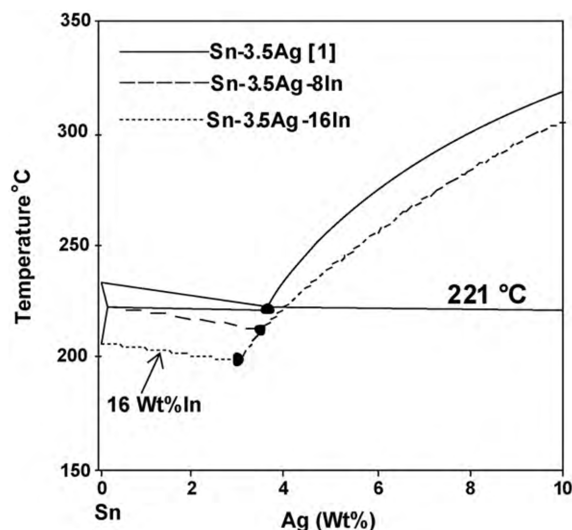

Fig. 2. The effect of In on the eutectic temperature in the Sn–Ag phase diagram.

3.2. Microhardness

Microhardness value is to determine the hardness of individual grains and characterize the mechanical properties of the solid state surface. The results obtained for microhardness values at small load (25 g) of the pure metals Sn, Ag, In, and the Sn solder alloys at room temperature are shown in Table 2. As seen from the table, the average hardness values decreases significantly with increasing the amount of indium, indicating that the bonding force between Ag and Sn is much stronger than that of indium and Ag or Sn. In addition, such a decrease in hardness value is generally taken as indicative of inhomogeneity of the system. Hence, the variation in hardness is attributed to the structural changes of the matrix phase.

In a previous work [4] it was found that In addition to Sn–3.5Ag resulted in a decrease of hardness and an increase of the thermal stability of the solder alloy.

3.3. Creep results

Under usual operating conditions, the temperature of solder joints in the microelectronic packages ranges between 298 and 373 K, which corresponds to quite a high homologous temperature (0.6–0.8 T_m). In this temperature range, creep is the most important deformation mechanism [11].

Isothermal creep test for Sn solder alloys (Sn–3.5Ag–8In and Sn–3.5Ag–16In), initially annealed for 1 h at 324 ± 2 K is carried out at five constant applied stresses (5.1, 5.8, 5.4, 6.2 and 6.6 MPa) and five test temperatures (443, 453, 463, 473, and 483 K).

Table 2
Room temperature Vickers hardness number (in units of N/mm^2) of the pure metals and Sn solder alloys.

Type	Samples (wt.%)	HV. at R.T. (N/mm^2)
Pure metals	Sn	79.5
	Ag	895.7
	In	95
Alloys	Sn–3.5Ag [1]	125
	Sn–3.5Ag–8In	119
	Sn–3.5Ag–16In	98

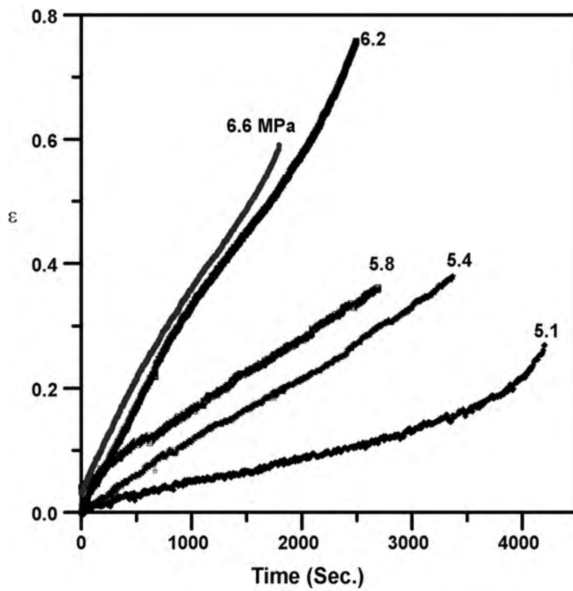

Fig. 3. Example of isothermal creep curves for Sn–3.5Ag–8In ternary alloy under different stresses and at 324 K annealing temperature for (1 h).

Generally, mechanical creep of a soldering material occurs more readily when elevated temperatures are involved. At elevated temperature, the mechanical properties of metals are a result of simultaneous processes of strain hardening, due to plastic deformation, and the softening effect of recovery and recrystallization [7].

Figs. 3 and 4 show typical isothermal creep curves for the Sn–3.5Ag–8In and Sn–3.5Ag–16In alloys at 443 K test temperature. The creep behavior observed at low temperature has three characteristic stages. A region of initial (unsteady) creep, in which the rate of creep varies rapidly followed by a region in which the rate of creep remains constant (steady state) creep and finally a third region in which the rate of creep increase rapidly which is followed by failure, as shown in Figs. 5 and 6.

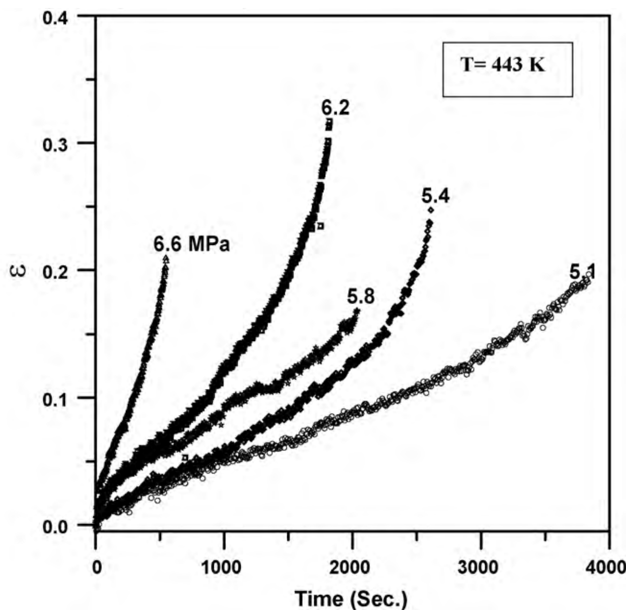

Fig. 4. Example of isothermal creep curves for Sn–3.5Ag–16In ternary alloy under different stresses and 324 K annealing temperature for (1 h).

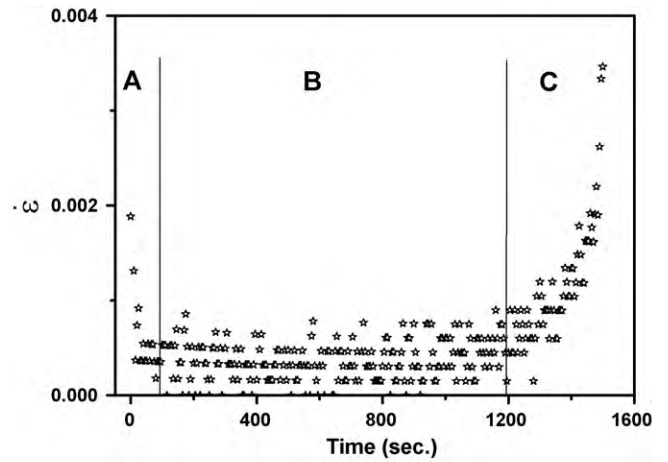

Fig. 5. Example creep rate curve for Sn–3.5Ag–8In ternary alloy showing different stages of the creep behavior at 445 K and strees 5.4 MPa. A, the transient state interval; B, the steady state interval; C, the tertiary state interval.

3.3.1. The steady state creep rate

The steady state creep rate $\dot{\varepsilon}_s$ calculated from the slopes of the linear regions of the creep curves, increases with increasing applied stresses and test temperature. The variation in strain rates (creep rates) is the result of changes in the internal structure of the material with creep strain and time.

Furthermore the steady state creep time can be determined from interval B for Sn–3.5Ag–8In and –3.5Ag–16In solder alloys (Figs. 5 and 6). The tensile strength on the other hand of Sn alloys is strongly influenced by strain rate similar to other lead-free solders [12,13]. The relationship of stress–strain of Sn solder alloys is usually expressed by the following equation within the steady state region (B):

$$\dot{\varepsilon}_s = A\sigma^{\,n} \tag{1}$$

where A is a constant and n is the stress exponent. A plot of logarithm of $\dot{\varepsilon}_s$ versus the logarithm of σ yields a straight curve with slope (n) which determines the mechanism of creep deformation.

A commonly used equation by design engineers for stress and temperature dependence of creep (strain) rate, especially in the electronics industry, is the Norton power law [13]:

$$\dot{\varepsilon}_s = A\sigma^n e^{-Q/RT} \tag{2}$$

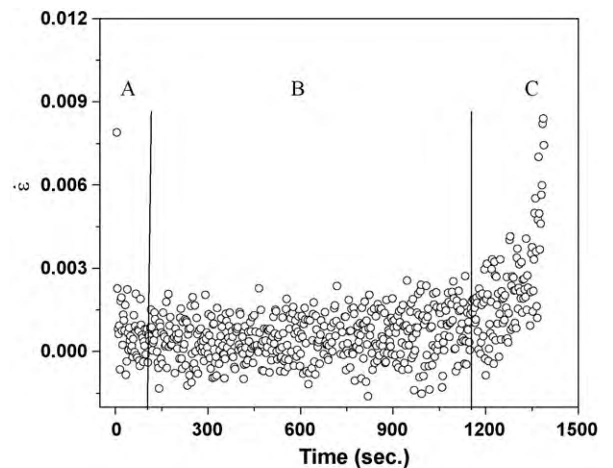

Fig. 6. Example creep rate curve for Sn–3.5Ag–16In ternary alloy showing different stages of the creep behavior at 445 K and strees 5.4 MPa. A, the transient state interval; B, the steady state interval; C, the tertiary state interval.

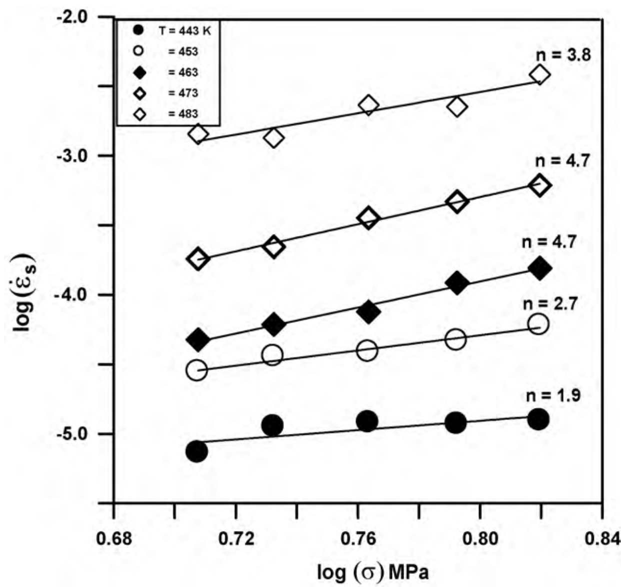

Fig. 7. Double-log of minimum creep rate versus stress at different test temperature for (Sn–3.5Ag–8In) ternary alloy.

where $\dot{\varepsilon}_s$ is the steady state strain rate, A is a constant, σ is the stress, n is the stress exponent, Q is the activation energy, R is the universal gas constant, and T is the absolute temperature. The stress exponent (n) determines the type of deformation mechanism (viscous glide, screw dislocation, climb mechanism, etc.). The transition from viscous glide (stress exponent $n \approx 3$) to dislocation climb (stress exponent $n \geq 4$).

The relation between log $\dot{\varepsilon}_s$ and log σ according to Eq. (1) is shown in Figs. 7 and 8 for Sn–3.5Ag–8In and Sn–3.5Ag–16In solder alloys respectively. The values of $\dot{\varepsilon}_s$ increased with increasing the applied stress and/or the test temperature for both alloys. The increase of $\dot{\varepsilon}_s$ with increasing test temperature could be explained in view of an easier motion of dislocations already existing, where the thermal energy introduced facilitates the dislocation motion by helping it to overcome the precipitates which act as barriers [14,15].

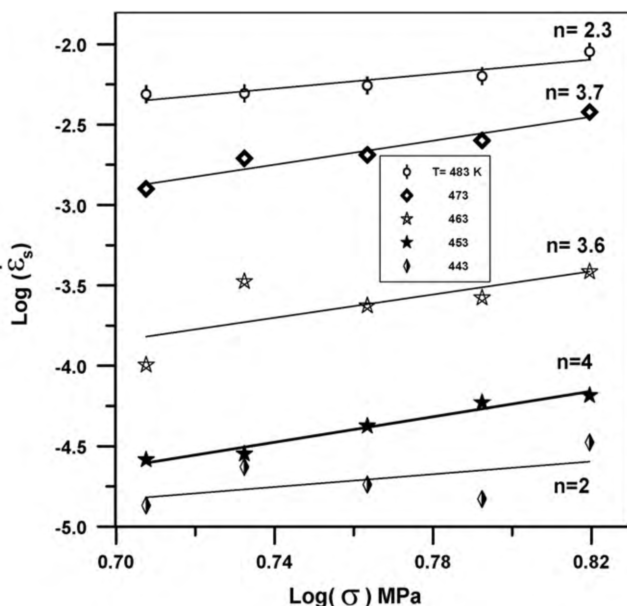

Fig. 8. Double-log of minimum creep rate versus stress at different test temperature for (Sn–3.5Ag–16In) ternary alloy.

Table 3
The stress exponent n for Sn solder alloys at different test temperature.

Sample	Test temperature	Exponent n (present)	Load (MPa)
Sn–3.5Ag–8In	443	2.3	6.6
	453	3.7	6.2
	463	3.6	5.4
	473	4	5.1
	483	2	5
Sn–3.5Ag–16In	443	3.8	6.6
	453	4.6	6.2
	463	4.6	5.4
	473	2.7	5.1
	483	2	5

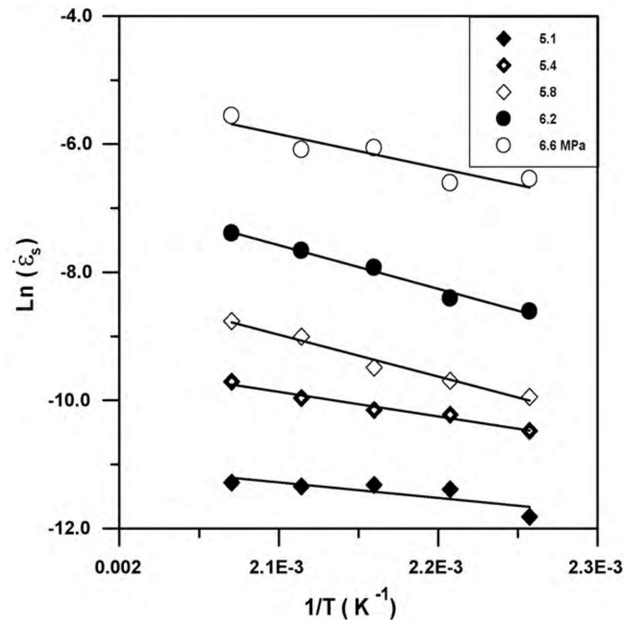

Fig. 9. Relation between ln $\dot{\varepsilon}_s$ and $1/T$ (K^{-1}) for (Sn–3.5Ag–8In) ternary alloy at different applied stresses.

The values of the stress exponent n for Sn–3.5Ag–8In and –3.5Ag–16In solder alloys (Figs. 7 and 8) depend mainly on the test temperature with values between 2 and 4.6. In addition, the deformation mechanisms in these alloys are viscous glide and dislocation climb according to the value of n given in Table 3.

The activation energy of the steady state creep of the alloy calculated according to Eq. (2) from the slopes of the relation between ln $\dot{\varepsilon}_s$ and $10^3/T$ is found to be linear for all applied stresses for Sn–3.5Ag–8In and Sn–3.5Ag–16In solder alloys as shown in Figs. 9 and 10 respectively. Tables 4a and 4b show the present activation energy value of Sn–3.5Ag–In and Sn–3.5Ag–16In solder alloys which were calculated from Figs. 8 and 9, is controlled by volume self diffusion [16].

Table 4a
The activation energy from the steady state creep at different stresses for Sn solder alloy.

Sample	Stress (MPa)	Activation energy (ev)	Average activation energy (ev)
Sn–3.5Ag–8In	6.6	0.26	0.34
	6.2	0.44	
	5.4	0.44	
	5.1	0.46	
	5	0.23	

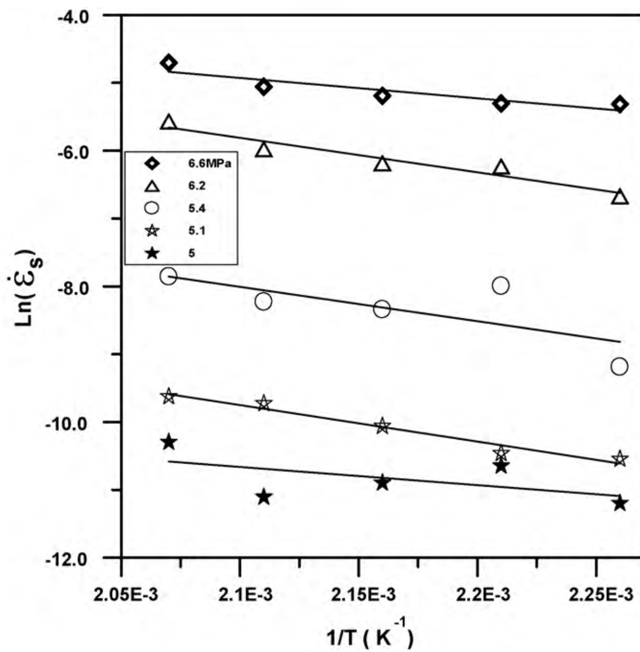

Fig. 10. Relation between ln $\dot{\varepsilon}_s$ and $1/T$ (K^{-1}) for (Sn–3.5Ag–16In) ternary alloy at different applied stresses.

The steady state creep activation energy of Sn–3.5 wt.%Ag alloy could be equal to either pure Sn (particularly in the case of rode-like microstructure), or being higher in case of dispersed intermetallic. According to the data presented in the mechanical behavior of Sn–3.5 wt.%Ag solder alloy is affected by Ag3Sn intermetallics precipitation [2]. From the discussion in Ref. [12] it is clear that due to the presence of intermetallic precipitates, the activation energy for Sn–3.5 wt.%Ag alloy creep should be higher than for pure Sn.

4. Microstructure

Sn–Ag alloys are being considered as one of the most favorable lead-free solder systems. In this respect numerous studies have been devoted to the microstructure of Sn–Ag based alloys [17–21]. Knowing that a nonequilibrium eutectic transformation occurs during the solidification of Sn–Ag eutectic alloy and thus the β-Sn dendrites and Sn–Ag3Sn eutectic coexist in the microstructure. Microstructure of SnAgIn was irregular, with fine Sn dendrites, eutectic, and coarse structural regions.

Figs. 11 and 12 show the microstructure before and after creep test with 94.5% cold work at annealing temperature 324 ± 2 K for 1 h. The plastic deformation of the alloys is because of cold work Figs. 11a and 12a of the Sn–3.5Ag–8In and Sn–3.5Ag–16In solder alloys. The cold deformation fragmented the dendrites and oriented them linearly. The effect of high degree of deformation after creep test on the microstructure of the alloy, where the block size is very large, is shown by more elongation of the grains than before the creep test. The structure after creep contains AgIn-γ, Ag3Sn phase [22,23] and β Sn dendrites, which are aligned to the tensile axis but the structure is less oriented before tensile deformation (Figs. 11b and 12b).

As shown in Fig. 11b the micrograph after low-temperature annealing at 324 K and after the creep test at stress of 5.4 MPa dif-

Table 4b
The activation energy from the steady state creep at different stresses for Sn solder alloy.

Sample	Stress (MPa)	Activation energy (ev)	Average activation energy (ev)
Sn–3.5Ag–16In	6.6	0.46	0.42
	6.2	0.57	
	5.4	0.55	
	5.1	0.33	
	5	0.21	

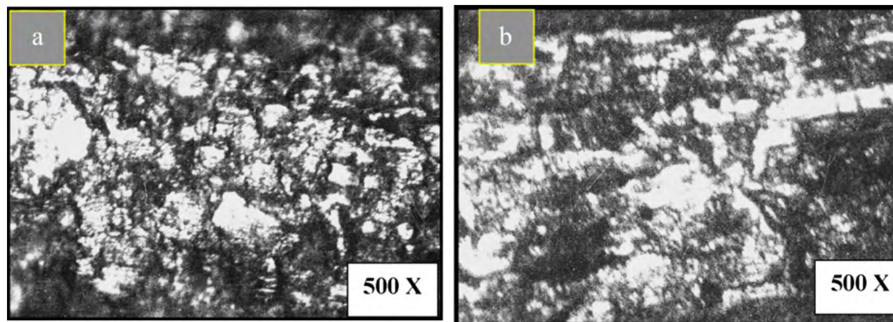

Fig. 11. Microstructure of Sn–3.5Ag–8In alloy (a) before and (b) after creep test.

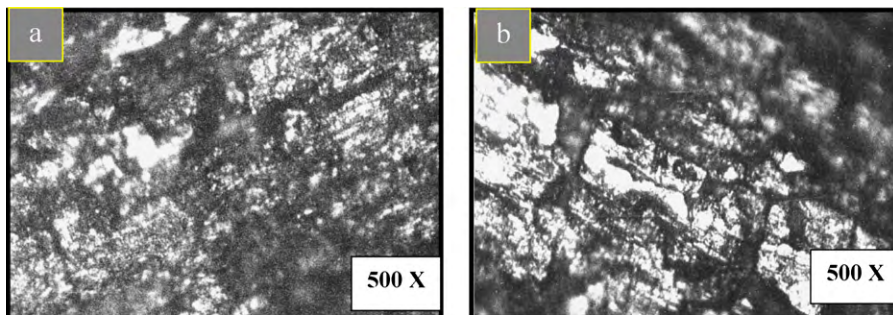

Fig. 12. Microstructure of Sn–3.5Ag–16In alloy (a) before and (b) after creep test.

fers in grain size from that in Fig. 11a, where deformation shows considerable coarsening of the grains [24]. The density decrease of the Sn–Ag intermetallic particles within the matrix is due to grain-boundary segregation and/or dissolution of the SnAg intermetallic.

5. Conclusion

Based on DTA curve, the information on characteristic peak temperatures of investigated Sn–Ag–In alloys (with high percent of tin, small percent of silver and indium) were obtained. DTA curves indicate that the beginning and the end of phase transformation are moved to lower temperature by the increase of indium and constant silver content in the alloy.

Microhardness measurements on the pure Sn, Ag, In and Sn–Ag–In alloys at small load were measured at room temperature. It is found that In addition to Sn–3.5Ag resulted in a decrease of hardness and an increase of the thermal stability of the solder alloy.

From steady state stage, the values of the stress exponent n is governed by viscous glide and dislocation climb, where the n values are in the range from 2 to 4.6. Values of activation energy of the mechanisms operating in the steady state stages were found in the range of 0.34 and 0.42 eV for the Sn–3.5Ag–8In and Sn–3.5Ag–16In solder alloys.

The microstructure of Sn–3.5Ag–8In and Sn–3.5Ag–16In alloys after creep test shows that block size is very large and the grain is elongated.

References

[1] M.M. EL-Bahay, M.E.L. Mossalamy, M. Mahdy, A.A. Bahgat, J. Mater. Sci.: Mater. Electron. 15 (2004) 519–526.
[2] D.R. Flanders, E.G. Jacobs, R.F. Pinizzotto, J. Electron. Mater. 26 (1997) 883.
[3] Report Lead-Free Solders NASA Part and Packaging Program Goddard Space Flight Center Greenbelt, Maryland 1996.
[4] A. Milosavlevic, D. zivkovic, Z. Kamberovic, Metalurgija—J. Metall. 14 (3) (2008) 161–167.
[5] Y. Lakhtin, Engineering Physical Metallurgy, Mir Publishers, Moscow, 1971, p. 53.
[6] M.M. EL-Bahay, E.L.M. Mossalamy, M. Mahdy, A.A. Bahgat, Phys. Status Solidi (a) 198 (2003) 76–90.
[7] A.A. Bahgat, M.M. El-Bahay, M.E. El-Mossalamy, M. Mahdy, Int. J. Pure Appl. Phys. 1 (1) (2005) 55.
[8] S. Atia, Ph.D. Thesis, Al-Azher University Faculty of Science, 2006.
[9] W.D. Callister Jr., Materials Science and Engineering, 3rd ed., John Wiley and Sons, New York, 1994, p.130.
[10] J.M. Song, Z.M. Wu, D.A. Huang, Scripta Mater. 56 (2007) 413–416.
[11] J. Yu, D.K. Joo, S.W. Shin, Acta Mater. 50 (2002) 4315–4324.
[12] V.I. Igoshev, J.I. Kleiman, J. Electron. Mater. 29 (2000) 244.
[13] D. Mitlin, C.H. Reader Jr., R.W. Messler, Metall. Trans. A 30 (1999) 115.
[14] M.A. Mahmoud, Phys. Status Solidi (a) 186 (2001) 143.
[15] W.A. Wood, The Study of Metal Structure and Their Mechanical Properties, Pergamon Press, New York, 1971.
[16] M.S. Sakr, A.Z. Mohamed, A.A. El-Daly, A.M. Abdel-Daiem, A.H. Bassyouni, Egypt. J. Sol. 13 (1990) 34.
[17] C.M. Miller, I.E. Anderson, J.F. Smith, J. Electron. Mater. 23 (1994) 595.
[18] M.L. Huang, L. Wang, Metall. Mater. Trans. A 36 (2005) 1439.
[19] L.P. Lehman, S.N. Athavale, T.Z. Fullem, A.C. Giamis, R.K. Kinyanjui, M. Lowenstein, K. Mather, R. Patel, D. Raw, J. Wang, Y. Xing, L. Zavalij, P. Borgesen, E.J. Cotts, J. Electron. Mater. 33 (2004) 1429.
[20] S.K. Kang, W.K. Choi, D.Y. Shih, D.W. Henderson, T. Gosselin, A. Sarkhel, C. Goldsmith, K.J. Puttlitz, JOM 55 (2003) 61.
[21] K.S. Kim, S.H. Huh, K. Suganuma, Microelectron. Reliab. 43 (2003) 259.
[22] W.K. Choi, J.H. Kim, S.W. Jeong, H.M. Lee, J. Mater. Res. 17 (2002) 43–51.
[23] J. Horo, P.G. Harne, B.B. Nayak, S. Vitta, Mater. Sci. Eng. 107 (2004) 53–57.
[24] R.K. Mahidhara, S.M. Sastry, I. Turlik, K.L. Murty, Scripta Metall. Mater. 31 (1994) 1145.